[7] Y. Feldman, E. Wasserman, D. J. Srolovitz, R. Tenne, *Science* **1995**, *267*, 222; L. Margulis, G. Salitra, R. Tenne, M. Talianker, *Nature* **1993**, *365*, 113.
[8] A recent review of fullerene structures in the metal-dichalcogenides is presented in R. Tenne, *Adv. Mater.* **1995**, *7*, 965.
[9] H. Kroto, *Science* **1988**, *242*, 1139.
[10] D. Ugarte, *Nature* **1992**, *359*,707.
[11] A. Thess, R. Lee, P. Nikolaev, H. Dai, P. Petit, J. Robert, C. Xu, Y. H. Lee, S. G. Kim, A. G. Rinzler, D. T. Colbert, G. E Scuseria, D. Tomanek, J. E. Fisher, R. E. Smalley, *Nature* **1996**, *273*, 483.
[12] S. Huang, *Proc. of Nanotube 99*, East Lansing, Michigan **1999**.
[13] S. N. Magonov, M. H. Whangbo, *Surface Analysis with STM and AFM: Experimental and Theoretical Aspects of Image Analysis*, VCH Weinheim, Germany **1996**

---

# Photodiodes Based on Polyfluorene Composites: Influence of Morphology**

By *Jonathan J. M. Halls, Ana C. Arias, J. Devin MacKenzie, Weishi Wu, Mike Inbasekaran, Ed P. Woo,* and *Richard H. Friend**

Semiconducting conjugated polymers for display applications are beginning to make the transition from laboratory to market place, while research continues into their use in applications including transistors, integrated optoelectronic devices,[1] voltage regulators,[2] solar cells, and photodiodes.[3] Research into novel materials, processing techniques, and device geometries have yielded exciting developments in stability, lifetime, and performance in all areas of application. For example, efficient photodiodes have been fabricated from mixtures of electron- and hole-accepting polymers.[4,5] These polymer composites, which are deposited by spin-coating from solution, contain a high surface area of dispersed interfaces at which photogeneration of charges is efficient. The morphology of the polymer mixture is crucial to the efficient operation of these devices. In this paper, we demonstrate directly and, to the best of our knowledge, for the first time, how the photocell performance can be controlled by manipulating the morphology of the polymer blend, which we achieve by controlling the rate of solvent evaporation during spin-coating.

Substituted polyfluorene-based polymers are an important example of a range of new highly-fluorescent semiconducting polymers. Poly(9,9-dioctylfluorene) was developed as a blue-emitting material for polymer light-emitting diodes (LEDs),[6] and has since been shown to exhibit non-dispersive hole transport with a relatively high mobility of $4 \times 10^{-4}$ cm$^2$ V$^{-1}$ s$^{-1}$.[7] The thermal stability and photostability of polyfluorenes has been shown to be considerably better than those of the phenylene–vinylene polymers.[8] Polyfluorene-based materials are expected to play an important part in the emissive displays of the future.

We have demonstrated previously that efficient photovoltaic devices can be fabricated from blends of semiconducting polymers with different electron affinities and ionization potentials.[4,9] Excitons photogenerated in the blend are dissociated by charge transfer of the electron to one component of the blend and hole transfer to the other component. This process of photogeneration was established in molecular semiconductors by Tang et al.[10] The interpenetrating network formed by a blend of two such polymers provides both the high surface area of spatially distributed interfaces necessary for efficient charge generation, and the means for separately collecting electrons and holes. While the probability of charge transfer at an interface in a binary blend is determined by the relative energy levels of the constituent polymers,[11] the morphology of the polymer composite plays an important part in determining the efficiency of a polymer blend photodiode.

The low entropy of mixing prevents miscibility of polymers on a molecular level, and they tend to phase separate into discrete domains.[12] In equilibrium, the lowest energy state is generally attained when the two components separate to form two bulk domains. When a thin film is prepared from a blend of polymers in solution by spin-coating, the solvent evaporates quickly, and an equilibrium state is rarely reached. Instead, phase separation occurs with domain sizes ranging from a few nanometers to several microns. The faster the solvent evaporates the less time the polymer has to rearrange itself into discrete domains from the intimate mixture that presumably exists in solution, leading to a finer-scale phase separation. We have previously established that the exciton diffusion range in poly(*p*-phenylenevinylene) (PPV) is of order 10 nm;[13] it is reasonable to assume that the diffusion range in the materials studied here is of the same order of magnitude. For the majority of photogenerated excitons to reach an active interface before decaying via an alternative route, the length-scale of the phase separation must be less than or equal to this diffusion range. A relatively fine-scale mixing is therefore favored for efficient photogeneration of charge carriers in a polymer composite photovoltaic cell.

We have demonstrated directly that the morphology of a polymer blend, and hence the properties of a photodiode using the blend film as an active layer, can be manipulated by control of the rate of solvent evaporation during spin-coating. In this paper, we demonstrate how the rate of evaporation may be increased by heating the substrate during spin-coating, and show how the resulting fine-scale phase separation leads to an increase in the quantum effi-

---

[*] Prof. R. H. Friend, Dr. J. J. M. Halls, A. C. Arias,
Dr. J. D. MacKenzie
Cavendish Laboratory
Madingley Road, Cambridge, CB3 0HE (UK)
Dr. W. Wu, Dr. M. Inbasekaran, Dr. E. P. Woo
Central and New Businesses R&D
Dow Chemical Company
Midland, MI 48674 (USA)

[**] This work has been partially supported by Dow Chemicals, USA and by the European Commission under Brite-Euram contract BRPR-CT97-0469. ACA thanks the Brazilian government for funding under a CNPq scholarship. We gratefully acknowledge the assistance of Cambridge Display Technology Ltd., and in particular Craig Murphy and Ellen Moons, in the provision of AFM equipment.

0935-9648/00/0704-0498 $ 17.50+.50/0

ciency of polymer composite photocells. Additional investigations, to be published separately, have shown that similar control may be achieved by spin-coating from different solvents, and by using different coating techniques.

The chemical structures of the two polyfluorene-based materials used in this investigation are shown in Figure 1a. F8BT is a stable luminescent polymer that emits green–yellow luminescence with a high efficiency.[14] PFB is a dioctylfluorene–triarylamine copolymer that has been shown to combine the high hole mobilities of molecular triarylamine glasses[10,15] with the processability advantages enjoyed by polymers. Hole mobilities of up to $2 \times 10^{-3}$ cm$^{2}$ V$^{-1}$ s$^{-1}$ have been reported by Redecker et al.[16] The large offset between the highest occupied molecular orbital (HOMO) and lowest unoccupied molecular orbital (LUMO) levels of the two polymers (0.8 eV and 1.24 eV respectively)[17] indicates that charge transfer of electrons from the PFB to the F8BT, and of holes in the opposite direction, is energetically favorable. This has been confirmed by the observation of photoluminescence quenching in this blend. It is for this reason, combined with their stability and the good hole transporting properties of PFB, that we employed this polymer system for this investigation. Solutions of the two polymers in xylene were mixed together, such that the ratio of F8BT to PFB was 1:1 by weight. Absorption spectra of thin spin-cast films of the two polymers, and of the blend, are presented in Figure 1b. The absorption of PFB is blue-shifted in comparison to F8BT. The absorption spectrum of the blend is a linear combination of those of its components, indicating that ground-state charge transfer does not occur in the mixture.

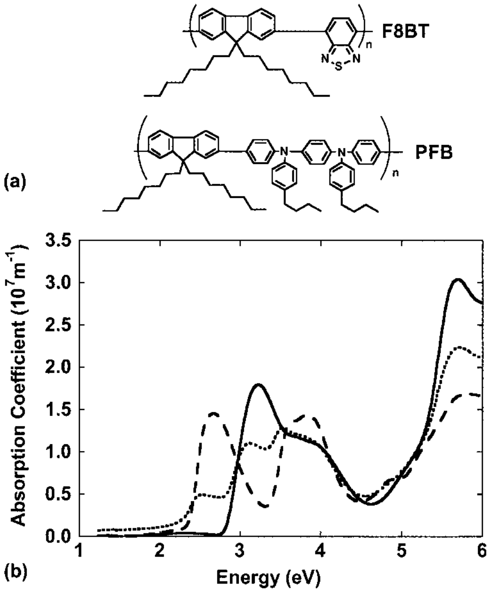

Fig. 1. a) Chemical structures of F8BT and PFB. b) Absorption spectra of thin films (10 nm) of F8BT (dashed line), PFB (solid line), and a PFB:F8BT blend (1:1 by weight) (dotted line). The films were prepared by spin-coating from solution in xylene onto quartz substrates.

Photovoltaic cells were fabricated with a single layer of polymer sandwiched between electrodes with different work functions. Indium tin oxide (ITO) coated glass was used as the transparent anode, over which the appropriate polymer solution was spin-coated, and aluminum was chosen for the cathode. Figure 2 shows the spectral dependence of the short-circuit photocurrent for devices made with the 1:1 polymer mixture and with the individual polymers. For these devices, spin-coating was carried out at room temperature using xylene as the solvent. The spectra have been corrected for the absorption of the ITO/glass substrate, which prevents photocurrent measurements at wavelengths below 320 nm. It can be seen that the blend photocell is considerably more efficient than the homopolymer cells across the whole spectral range. At 410 nm the photocurrent in the blend photocell is some 880 times higher than in the F8BT cell and 14 times greater than in the PFB device. The spectral response of the blend photocell broadly follows the quantity of light absorbed in the polymer layer, indicating that absorption of light throughout the polymer bulk contributes to the photocurrent. This, combined with our observation of the quenching of photoluminescence in the polymer blend, provides firm evidence for the dissociation of excitons at the interfaces distributed throughout the bulk of the composite. In contrast, the F8BT cell shows a response that increases steeply with increasing excitation energy; this has been rationalized by a theoretical analysis of the nature of the excited states in PPV and its derivatives.[18] In this model, excitons excited at higher energies have more delocalized wavefunctions and smaller binding energies, making them more likely to dissociate. The action spectrum of the PFB cell resembles more closely the absorption spectrum of the polymer, although the photocurrent is much lower than in the blend cell.

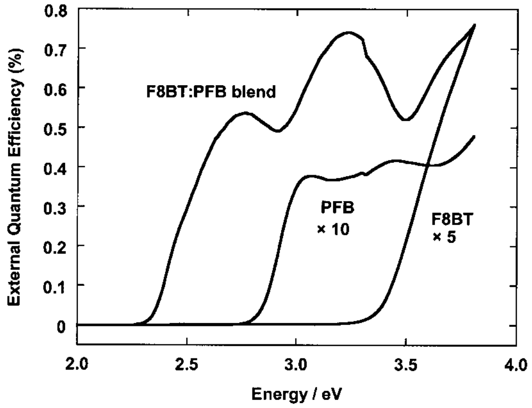

Fig. 2. Short-circuit photocurrent action spectra of photovoltaic cells fabricated from F8BT, PFB, and a 1:1 blend by weight of the two polymers. The quantum efficiency values for the two homopolymer photocells have been scaled by to make comparison with the blend cell easier. The action spectra have been corrected for the absorption spectrum of the ITO-coated glass substrate.

0935-9648/00/0704-0499 $ 17.50+.50/0

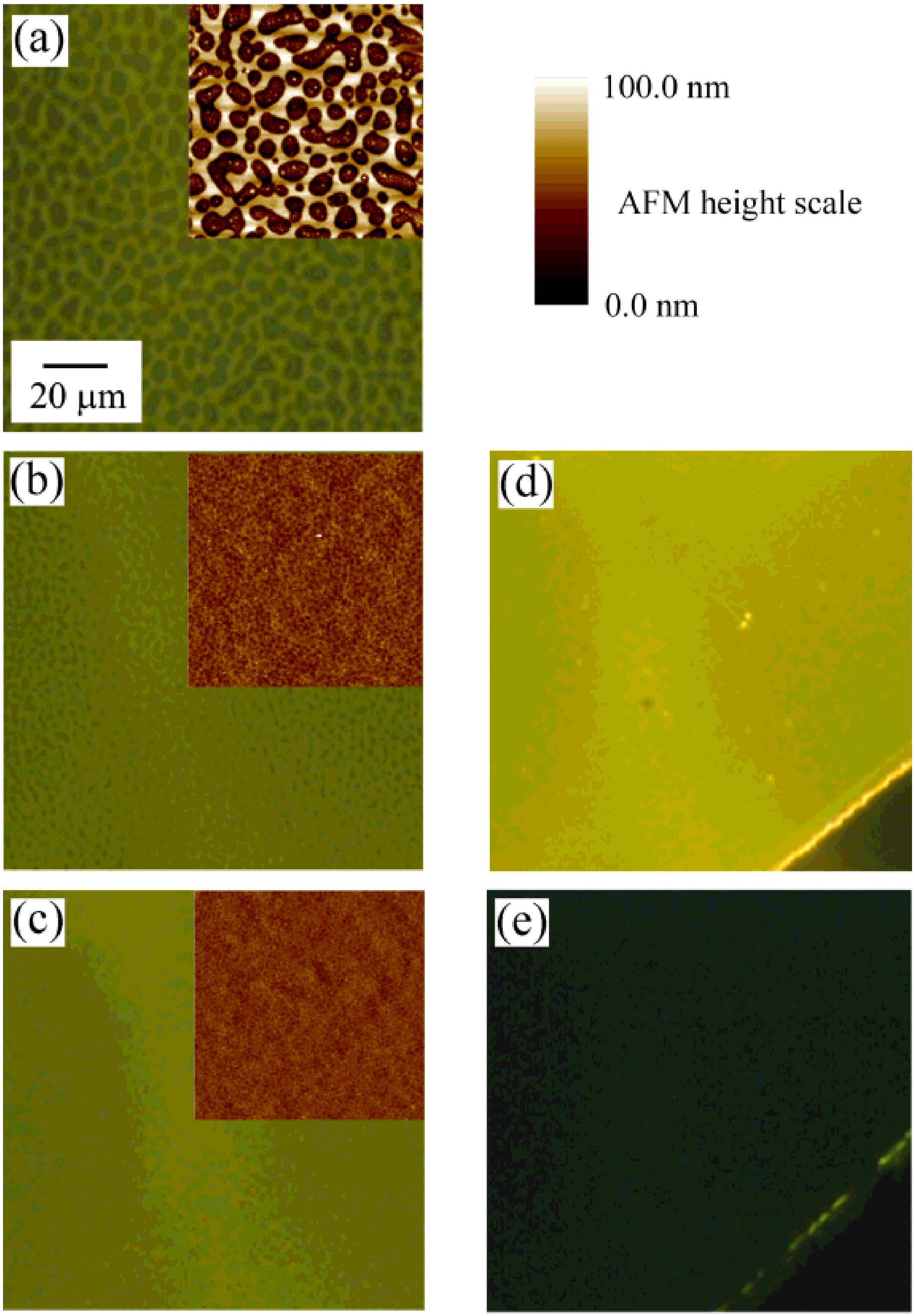

Fig. 3. a–c) Fluorescence microscopy images, with inset topographical AFM images of the F8BT:PFB polymer blend acquired at different positions on the substrates, associated with the regions marked A, B, and C in Figure 4. Image a) shows a region of coarse-scale phase separation, whereas image c) shows a region of mixing on a much finer scale than the resolution of the image. Image b) shows a region with phase separation on an intermediate scale. The AFM and fluorescence images both have the same in-plane scale. d,e) Fluorescence microscopy images of pristine films of F8BT (d) and PFB (e). The images have the same in-plane scale as Figures 3a to c.

To investigate the effect of increasing the solvent evaporation rate, we heated the ITO/glass substrate and metal spin-coater chuck with a halogen lamp immediately prior to spin-coating. The chuck was heated to a maximum temperature of 95 °C. Due to the asymmetry of the heating process, the substrate temperature was not constant across its surface, resulting in the development of a range of different morphologies across the substrate. The photovoltaic properties of the eight separate pixels distributed over the surface of the substrate were characterized. The quantum efficiencies (electrons collected per incident photon) were found to depend on the position of the pixel on the substrate, and ranged from 0.25 % to 0.52 % under monochromatic excitation at 500 nm.

Regions of coarse-scale phase separation in the polymer-blend layer were evident to the naked eye, owing to the scattering of light from features larger than the wavelength of light. In order to map the length-scale of the phase separation across the substrate, the quantity of light scattered from the film was estimated from a transmission measurement. Selected areas of the pixels were imaged through the transparent glass substrate with an optical microscope in reflection mode. The amount of light passing through the substrate and polymer layer, reflecting from the aluminum contact, and returning back through the polymer layer and substrate back up the microscope column was measured with a silicon photodiode ($I$). A low-pass filter with a 590 nm cut-off was inserted directly after the light source to prevent photoexcitation and subsequent luminescence of the polymer. A 600 nm bandpass filter, with a 10 nm full width at half maximum (FWHM) bandwidth was placed in front of the silicon photodiode to select the wavelength band for the transmission measurement. The experimental arrangement for this measurement is illustrated in the schematic inset in Figure 3d. Since the transmission was measured below the optical gap of the polymers, the variation of transmission from pixel to pixel should depend only on the amount of scattering from the polymer composite, and from ripples in the aluminum contact formed

0935-9648/00/0704-0500 $ 17.50+.50/0

by the underlying polymer topography. To calibrate these transmission measurements, an aluminum film, deposited by thermal evaporation onto glass, was imaged in the same way, and the amount of light collected by the photodiode was recorded ($I_0$). The measurements made for each pixel were divided by this calibration measurement, to give a fractional transmission ($I/I_0$) in the 600 nm band.

Figure 4 shows a plot of the photovoltaic EQE against the fractional transmission in the 600 nm band for each pixel. The graph indicates that the pixels with the highest EQE have the highest transmission (up to 85 %), and therefore the lowest quantity of scattering. The polymer composite layer of these pixels is therefore expected to be phase separated on a much smaller scale than is the case with the less efficient pixels, which have transmissions of less than 55 % owing to the coarse-scale phase separation.

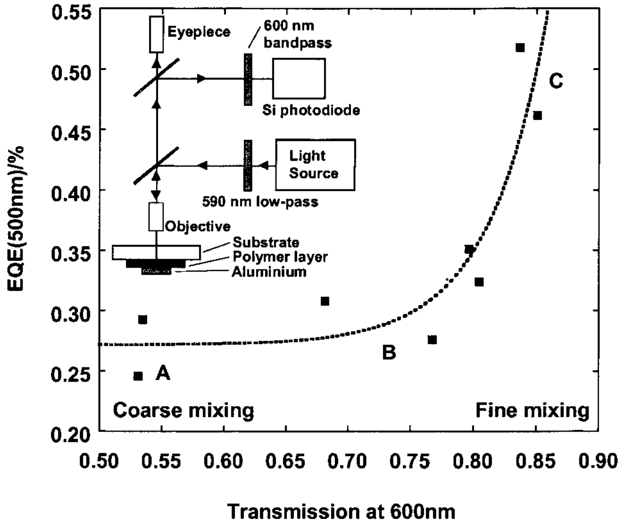

Fig. 4. Graph showing the relationship between the quantum efficiency and transmission of each of the eight pixels distributed across the substrate of the photodiode. The graph shows how the pixels with the highest transmission (i.e., lowest scattering and finest scale phase separation) have the highest quantum yields. The AFM images in Figure 3a–c were obtained in the vicinity of the pixels marked A, B, and C. The inset schematic diagram illustrates the experimental arrangement for the transmission measurement.

To confirm this interpretation, the morphology and local luminescence of the polymer composite film in the vicinity of the pixels was investigated with tapping-mode atomic force microscopy (AFM) and fluorescence microscopy. 50 μm × 50 μm AFM scans were performed at three different points over the film's surface. Fluorescence images of the same regions were obtained using an Hg illumination source with a pass filter transmitting plasma lines at 365 nm, 405 nm, and 435 nm. Light emitted with a wavelength greater than 505 nm was selected using a cut-off filter and imaged using a charge coupled device (CCD) array. In this way, the strongly luminescent F8BT component was selectively imaged as demonstrated in Figures 3d and 3e which show the luminescence contrast between F8BT and PFB homopolymer films, respectively. Figures 3a–c show fluorescence and (inset) AFM images from similar regions in the vicinity of the groups of photocell pixels marked A, B, and C in Figure 4. The AFM and fluorescence images are reproduced to the same scale. The inset image of Figure 3a shows the topography of the polymer film in region A, adjacent to the least efficient pixels. The morphology suggests the presence of two distinct phases distributed as islands of one phase in a continuous matrix of another. From the corresponding fluorescence image, it can be seen that PFB-rich areas form the isolated component, which is surrounded by an F8BT-rich phase. Through a grain-size analysis algorithm, the closed features shown in the AFM image were found to have a mean diameter of approximately 4.7 μm and a mean area of ~18 μm$^2$. This same area of the film demonstrated the highest amount of scattering and lowest EQE (0.25 % at 500 nm). In contrast, the image shown in Figure 3c, which was acquired in the vicinity of the least-scattering and most efficient pixels (region C) with an EQE of 0.52 % at 500 nm, does not show the same distinct micrometer-scale features, and the phase separation is clearly on a smaller scale. Grain-size analysis indicates a characteristic diameter of ~0.86 μm and area of ~0.58 μm$^2$ for the texture of this surface. Luminescence texture is only barely discernible in the fluorescence image for this region of the sample. The image displayed in Figure 3b, which was acquired near the pixels of intermediate efficiency (region B in Fig. 3), is similar in form to that of Figure 3c but with a somewhat larger grain size (mean diameter ~0.99 μm, mean area ~0.77 μm$^2$). Following the trend in phase-separation length scale, the EQE and scattering response of this area of the sample falls between that of regions A and C in Figure 4. The scale of the fluorescence features present in this region of the sample falls in between that of regions A and C as well. It is presumed that the scale of the composite phase separation varies with the local surface temperature and thus the solvent evaporation rate as a function of position on the sample surface; we have confirmed this by observing a range of composite films prepared at different temperatures.

In conclusion, we have demonstrated how the morphology of a polymer blend can be manipulated by control of the solvent evaporation conditions, and shown directly how the efficiency of a polymer composite photovoltaic cell can be enhanced by heating the substrate to increase the evaporation rate and reduce the length scale of the phase separation. Further work is in progress to optimize the morphology of thin-film polymer composites for photovoltaic applications, by employing different methods of controlling the rate of solvent evaporation.

## *Experimental*

Polymer solutions were prepared by dissolving the homopolymers (F8BT and PFB) separately in mixed xylenes at a concentration of 28 mg mL$^{-1}$. The blend solution was prepared by mixing equal quantities of these two solutions. Thin films for UV-vis absorption spectroscopy were prepared by spin-coating the appropriate solution onto quartz substrates. Photovoltaic devices were prepared by spin-coating from solutions onto ITO-coated glass substrates. In the case of the device prepared using a heated substrate, the spin-coater chuck and substrate was heated with radiation from a high intensity halogen lamp, which was extinguished immediately before spin-coating. Prior to coating, the substrates were cleaned in an ultrasonic bath with acetone and *iso*-propanol, and subsequently treated in an oxygen-plasma etcher to remove any remaining organic impurities. This treatment has also been shown to reduce surface roughness and increase the work function of the ITO. Aluminum contacts were deposited by thermal evaporation onto the polymer film. The active area of each pixel, defined by the overlap of the aluminum contacts with the patterned ITO, was 1 mm$^2$. The devices were fabricated in a nitrogen-filled glove box to reduce oxygen contamination.

The diodes were electrically characterized under a vacuum of order $10^{-7}$ mbar. For determination of the spectral response of the photocurrent, a xenon arc lamp, spectrally resolved by a monochromator, illuminated the diodes from the ITO side, at an intensity of order 0.1 mW cm$^{-2}$ at each wavelength interval. A Keithley 617 electrometer was used to measure the photocurrent. The spectral dependence of the power incident on the devices was measured by positioning a calibrated silicon photodiode in the sample position.

Tapping-mode AFM was carried out using a NanoScope IIIa Dimension 3100 (Digital Instruments Inc., Santa Barbara, CA). The quantity of scattering from different regions of the polymer film was quantified by imaging selected areas (approximately 0.5 mm$^2$ in area) with an optical microscope in reflection mode, and measuring the quantity of light reflected back down the microscope column with a silicon photodiode.

Received: September 28, 1999
Final version: January 17, 2000

---

[1] H. Sirringhaus, N. Tessler, R. H. Friend, *Science* **1998**, *280*, 1741.
[2] A. C. Arias, I. A. Hummelgen, A. Meneguzzi, C. Ferreira, *Adv. Mater.* **1997**, *9*, 972.
[3] M. Granstrom, K. Petritsch, A. C. Arias, A. Lux, M. R. Andersson, R. H. Friend, *Nature* **1998**, *395*, 257.
[4] J. J. M. Halls, C. A. Walsh, N. C. Greenham, E. A. Marseglia, R. H. Friend, S. C. Moratti, A. B. Holmes, *Nature* **1995**, *376*, 498.
[5] G. Yu, J. Gao, J. C. Hummelen, F. Wudl, A. J. Heeger, *Science* **1995**, *270*, 1789.
[6] A. W. Grice, D. D. C. Bradley, M. T. Bernius, M. Inbasekaran, W. W. Wu, E. P. Woo, *Appl. Phys. Lett.* **1998**, *73*, 629.
[7] M. Redecker, D. D. C. Bradley, M. Insbasekaran, E. P. Woo, *Appl. Phys. Lett.* **1998**, *73*, 1565.
[8] M. Kreyenschmidt, G. Klaerner, G. Fuhrer, J. Ashenhurst, S. Karg, W. D. Chen, V. Y. Lee, J. C. Scott, R. D. Miller, *Macromolecules* **1998**, *31*, 1099.
[9] J. J. M. Halls, R. H. Friend, *US Patent No. 5 670 791* **1997**.
[10] C. W. Tang, *Appl. Phys. Lett.* **1986**, *48*, 183.
[11] J. J. M. Halls, J. Cornil, D. A. dos Santos, R. Silbey, D.-H. Hwang, A. B. Holmes, J. L. Brédas, R. H. Friend, *Phys. Rev. B* **1999**, *60*, 5721.
[12] R. A. L. Jones, *Phys. World* **1995**, *8*, 47.
[13] J. J. M. Halls, K. Pichler, R. H. Friend, S. C. Moratti, A. B. Holmes, *Appl. Phys. Lett.* **1996**, *68*, 3120.
[14] Y. He, S. Gong, R. Hattori, J. Kanicki, *Appl. Phys. Lett.* **1999**, *74*, 2265.
[15] C. Giebeler, H. Antoniadis, D. D. C. Bradley, Y. Shirota, *Appl. Phys. Lett.* **1998**, *72*, 2448.
[16] M. Redecker, D. D. C. Bradley, M. Inbasekaran, W. W. Wu, W. P. Woo, *Adv. Mater.* **1999**, *11*, 241.
[17] W. Wu, M. Inbasekaran, E. P. Woo, personal communication **1999**.
[18] A. Köhler, D. A. d. Santos, D. Beljonne, Z. Shuai, J. L. Brédas, R. H. Friend, S. C. Moratti, A. B. Holmes, A. Kraus, K. Müllen, *Nature* **1998**, *392*, 903.

---

## Polymer–Gel Templating of Porous Inorganic Macro-Structures Using Nanoparticle Building Blocks[**]

By *Michael Breulmann, Sean A. Davis, Stephen Mann,*[*] *Hans-Peter Hentze,* and *Markus Antonietti*

The synthesis of hierarchically-ordered inorganic frameworks is of potential interest in various fields including catalysis,[1] separation techniques,[2] and materials chemistry.[3] Recently, there has been considerable interest in the use of surfactant and block copolymer mesophases as extended templates for the formation of monolithic composite materials.[4] Removal of the template by calcination produces a highly ordered porous inorganic replica of the interstitial spaces. Bicontinuous polymeric gels have also been used in a similar way as templates for the in-situ mineralization of magnetite[5] and titanium alkoxide polymerization.[6] In general, these strategies use molecular precursors that infiltrate and react within confined but structured spaces patterned by the polymeric template. For nano- and meso-scale structures, this approach generally works well, provided that there is sufficient chemical and interfacial complementarity between the organic and inorganic components. However, inorganic mineralization of ordered structures extending beyond 100 nm can be difficult to achieve at high volume fractions because the supersaturation level attainable within the template is too low to produce a stable replica of the void space. One possibility is to use flow, rather than batch processing; for example, the continuous flow of reactants through a latex colloidal crystal "membrane" has been used to construct inorganic frameworks with coherent micrometer-scale organization.[7] Another approach is to use larger-scale building blocks, such as preformed inorganic nanoparticles, in conjunction with physical and structural properties of the template that enable high infiltration, compaction and consolidation. For example, we previously showed that the reversible swelling of bacterial threads subjected to hydration and dehydration, could be used to prepare ordered macroporous inorganic fibers from aqueous colloidal sols

---

[*] Prof. S. Mann, Dr. M. Breulmann, Dr. S. A. Davis
University of Bristol
School of Chemistry
Bristol BS8 1TS (UK)

Prof. M. Antonietti, Dr. H. P. Hentze
Max Planck Institute for Colloids and Interfaces
Am Mühlenberg, D-14476 Golm (Germany)

[**] We thank Ursula Potter (University of Bath) for help with the low temperature SEM, Alex Kay for synthesis of the titanium dioxide colloids and Dr. Walther Schwarzacher (University of Bristol) for magnetic measurements. Financial support by the Max Planck Society, Leverhulme Trust and EPSRC is gratefully acknowledged. We thank the DAAD for a NATO postdoctoral fellowship to Dr. Michael Breulmann.

0935-9648/00/0704-0502 $ 17.50+.50/0